Single-cell Electrochemical Aptasensor Array

Shuo Li[*,†], Yannick Coffinier[‡], Chann Lagadec[§], Fabrizio Cleri[‡], Katsuhiko Nishiguchi[⁋], Akira Fujiwara[⁋], Soo Hyeon Kim[†] and Nicolas Clément[*,†]

† IIS, LIMMS/CNRS-IIS IRL2820, The Univ. of Tokyo 4-6-1 Komaba, Meguro-ku Tokyo, 153-8505, Japan
‡ IEMN, CNRS UMR8520, Univ. Lille Avenue Poincaré, BP 60069, 59652 Villeneuve d'Ascq cedex, France
§ Univ. Lille, CNRS, Inserm, CHU Lille, Centre Oscar Lambret, UMR9020 – UMR-S 1277 - Canther – Cancer Heterogeneity, Plasticity and Resistance to Therapies, F-59000 Lille, France
⁋ NTT Basic Research Laboratories, NTT Corporation, 3-1, Morinosato-Wakamiya, Atsugi-shi, 243-0198, Japan

KEYWORDS Bioelectrochemistry, Aptasensors, Single-cell, Nanopillars, EpCAM

ABSTRACT: Despite several demonstrations of electrochemical devices with limits of detection (LOD) of 1 cell/mL, the implementation of single-cell bioelectrochemical sensor arrays has remained elusive due to their challenging implementation at large scale. Here, we show that the recently introduced nanopillar array technology combined with redox-labelled aptamers targeting epithelial cell adhesion molecule (EpCAM) is perfectly suited for such implementation. Combining nanopillar arrays with microwells determined for single cell trapping directly on the sensor surface, single target cells are successfully detected and analyzed. This first implementation of a single-cell electrochemical aptasensor array based on Brownian-fluctuating redox species opens new opportunities for large-scale implementation and statistical analysis of early cancer diagnosis and cancer therapy in clinical settings.

The need for single cell detection and analysis techniques has increased in the past decades because of the heterogeneity of individual living cells, which increases the complexity of the pathogenesis of malignant tumors.[1-3] In the search for early cancer detection, high-precision medicine and therapy, the technologies most used today for sensitive detection of target analytes and monitoring the variation of these species are mainly including two types. One is based on the identification of molecular differences at the single-cell level, such as flow cytometry, fluorescence-activated cell sorting, next generation proteomics, lipidomic studies,[4-7] another is based on capturing or detecting single tumor cells from fresh or fixed primary tumors and metastatic tissues, and rare circulating tumors cells (CTCs) from blood or bone marrow, for example, dielectrophoresis technique,[8] microfluidic based microposts chip,[9] electrochemical (EC) approach. Compared to other methods, EC sensors have the merits of easy operation, high sensitivity, and portability.[10-19] For example, a recent technique using rolling circle amplification with aptamers could successfully demonstrate a limit of detection (LOD) as low as 5 CTC cells in whole blood (with 200 µL of the sample used for incubation).[20] Another approach using quantum dots as sensing probe attained a LOD of 2 cells/mL in human serum.[21] Very recently, PEDOT:PSS organic electrochemical transistors have shown the potential for electrical cell-substrate impedance sensing down to single cell.[22, 23] However, despite various demonstrations of low LOD including aptamer sensors,[21, 24, 25] arrayed EC sensors for detecting single-cell have not been demonstrated. Recently, we have introduced a new technique based on 20-nm-thick nanopillars array to support cells and keep them at ideal recognition distance for redox-labelled aptamers grafted on the surface. The key advantages of this technology are not only to suppress the false positive signal arising from the pressure exerted by all (including non-target) cells pushing on the aptamers by downward force, but also to stabilize the aptamer at the ideal hairpin configuration thanks to a confinement effect.[26] With the first implementation of this technique, a LOD of 13 cells (with 5.4 µL of cell suspension) was estimated.

In this work, the nanosupported cell technology using redox-labelled aptasensors has been pushed forward and fully integrated in a single-cell electrochemical aptasensor array. To reach this goal, the LOD has been reduced by more than one order of magnitude by suppressing parasitic capacitive electrochemical signals through minimizing the sensor area and localizing the cells. A statistical analysis at the single-cell level is demonstrated for the recognition of cancer cells. The future of this technology is discussed and the potential for scaling over millions of electrodes, thus pushing further integration at sub-cellular level is highlighted. A description of the experimental methods is reported in the Supplementary Materials.

Figure 1 shows a simple description of the operation of this single-cell EC aptasensor and the configuration of the proposed microfluidic system. The device is assembled on micrometric gold working electrodes; an active biorecognition monolayer, composed of tethered ferrocene (Fc)-labelled ssDNA SYL3C aptamers[24, 25] immobilized on the gold surfaces for the efficient and specific recognition of the epithelial cell adhesion molecules (EpCAMs), and the backfilling of oligoethylene glycol (OEG) molecules for mitigating nonspecific adsorption and stabilizing aptamers; a regular array of hydrogen-silsesquioxane (HSQ) nanopillars fabricated by high-speed e-beam lithography,[26, 28, 29] and SU-8 microwells for gravitationally trapping single-cell (the optical image and dimensions of the SU-8 microwells are shown in Figure S1). A simple description of the fabrication process is depicted in Figure 1c (more details are depicted in Figure S2). The choice of the dimensions of HSQ nanopillars was discussed in the previous work.[26] The atomic force microscopy (AFM) image shown in Figure 1d presents the HSQ nanopillars with a diameter of 200 nm, a height of 19.7 nm,

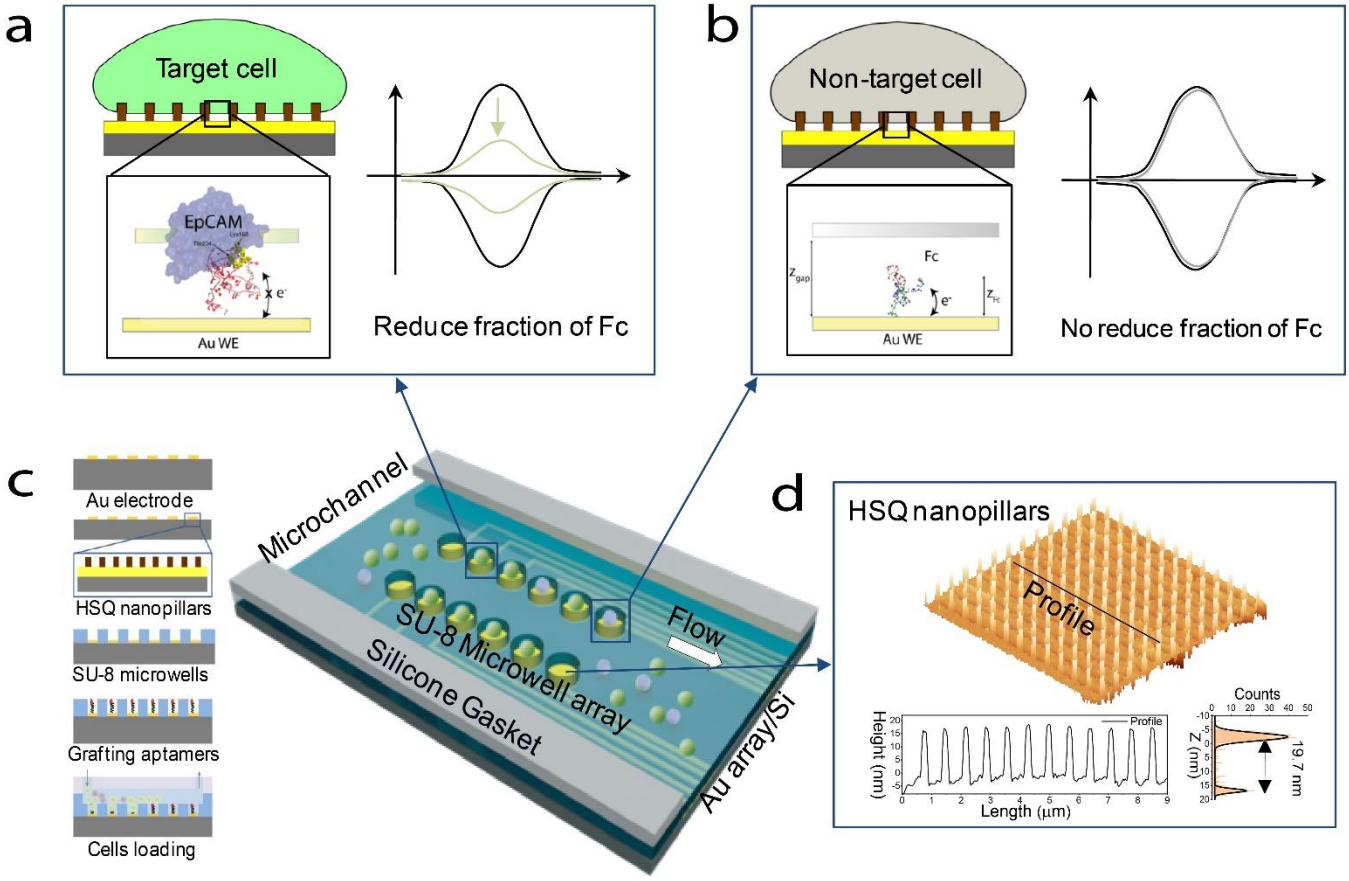

Figure 1. (a) Schematic representation of the nanopillars device used for the molecular recognition of EpCAM on a target cell by the SYL3C aptamer, and the relative CV with(black)/without (green) target cell. (b) Schematic representation of the device composed of a gold electrode with nanopillars supported a non-target cell, a tethered SYL3C-Fc aptamer, as well as the relative CV with (black)/without(grey) non-target cell. (c) Schematic to show the principle of electrochemical aptasensors for single cell analysis. (d) AFM image (10 μm × 10 μm) and AFM cross-section of the HSQ nanopillars.

pitch of 500 nm (a larger scale of the AFM of HSQ nanopillars that are well aligned on the Au microelectrode is shown in Figure S3); this configuration aimed to keep the cell at a distance z_{gap} of a few nanometers above the sensor surface, which is small enough to enable an interaction between the SYL3C aptamers and EpCAMs (Figure 1b), this z_{gap} has been estimated to be around 5 nm, upon consideration of cells deformation.

When the cells are seeded in the microfluidic device and incubated for a short time, each single cell will be gravitationally trapped in the microwell. In the presence of a target cell, the aptamer can get partly bond to the EpCAMs, and the fluctuations become more constrained. During the molecular recognition interaction, a number of H-bonds are formed between the second hairpin of the aptamer and a selected set of EpCAM residues, notably the Lys168 and the Thr234 (Figure 1b). Since the probability of charge transfer is proportional to the exponential of the distance (z_{gap}), the interaction of aptamer and EpCAM drastically reduces the electron transfer rate and the expected decrease of current is shown in Figure 1a. Therefore, the peak amplitude (I_{peak}) decrease can be related statistically to the percentage of aptamers interacting with the cell, a process that is thermally activated by the formation of H-bonds. In contrast, when there is no cell or in the presence of nontarget cell, the aptamers move freely, the Fc moves in a reproducible way on long enough time constants (>>10 microseconds). In this way, electron transfer between the surface and redox markers is allowed, therefore, no reduction of the fraction of Fc is expected, *i. e.* the cyclic voltammetry curves (CVs) keep the same with/without nontarget cell (Figure 1a).

The area of the voltammogram (related to either oxidation or reduction) represents the total charge transferred per cycle times the sweep rate. Therefore, it is directly related to the fraction of the aptamers on the surface that can effectively transfer the charge, and the I_{peak} is the key parameter to monitor. If the sweep rate is faster than the electron transfer or molecular diffusion rates, the shape of the voltammogram asymmetrically varies according to the oxidation/reduction peak potential.[30-32]

To check the improvement of the sensitivity of the nano-supported cells aptasensors by scaling down the sensing area (~700 μm^2) from large scale sensing area (36mm^2) and single cell, two types were developed. Figure 2a and 2b show the fluorescent images and the associated CVs in

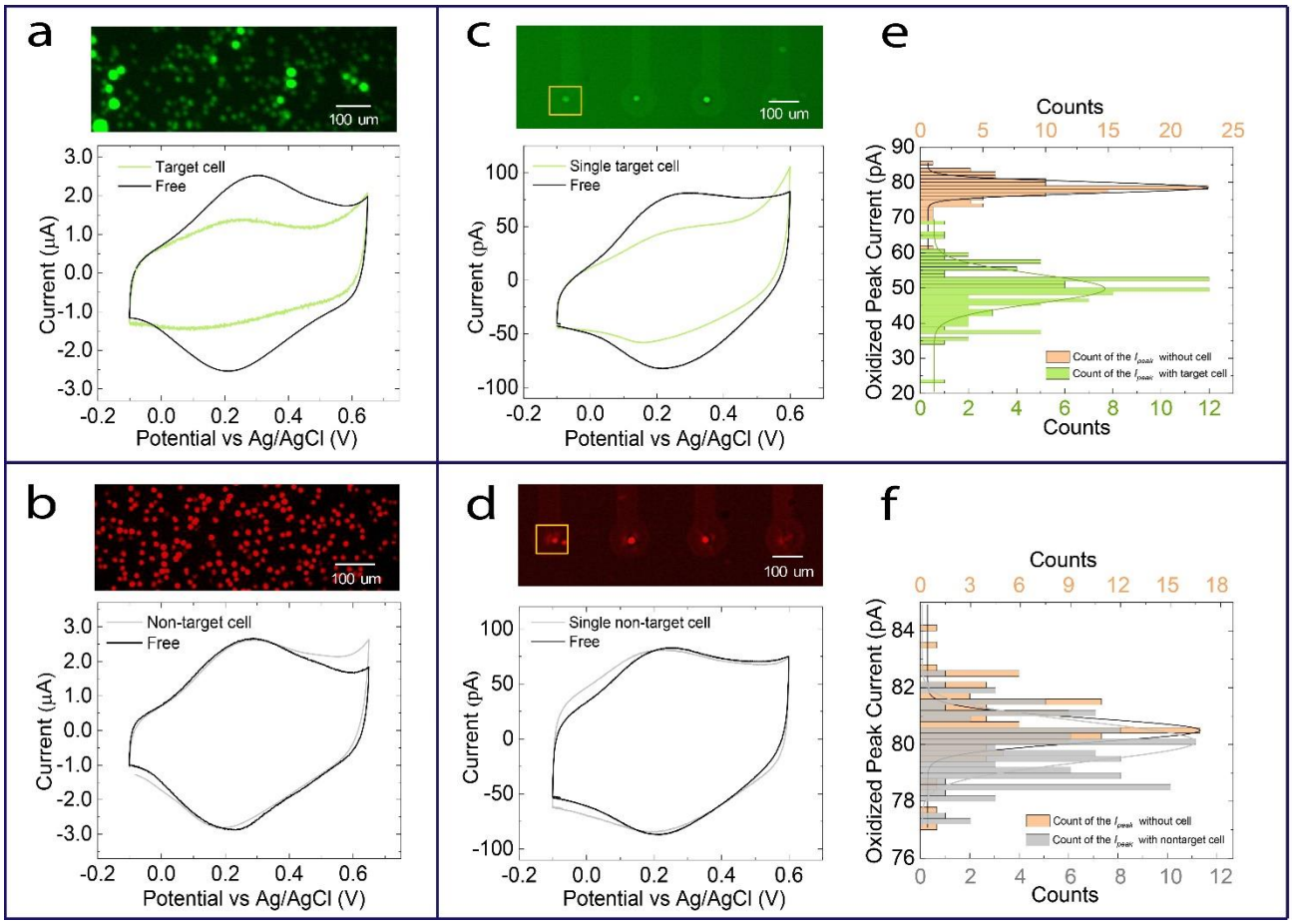

Figure 2. (a) Fluorescent image of target cell on the device with large-area surface and CVs (scan rate v = 0.5 V/s) in the presence/absence of target cells. (b) Florescent image of non-target cell on the device with large-area surface and CVs (v = 0.05 V/s) of a device in the presence/absence of non-target cells. (c) Fluorescent image of one target cell on the device with small-area surface and CVs (v = 0.5 V/s) in the presence/absence of one target cells. (d)Fluorescent image of one non-target cell on the device with small-area surface and CVs (v = 0.05 V/s) in the presence/absence of target cells. (e) Statistic of oxidation I_{peak} of 100 devices for detecting single target cell. (f) Statistic of oxidation I_{peak} of 100 devices for detecting single non-target cell.

absence/presence cell with larger surface sensing area. Here the lymphoma cell line Ramos was used as control experiment, which does not express EpCAM.[33] The pancreatic cancer cells (Capan-2) were detected as target cells, which have a high level of EpCAM expression.[34] The cell viability, cell number and size were determined using a Petroff-Hausser Vcell counting chamber before the detection, as shown in Figure S4. We observed a large shift in I_{peak} with 65% decrease in the presence of Capan-2 labelled with green color (Figure 2a) while no change for the I_{peak} in the control experiment, here Ramos are labelled with red color (Figure 2b), showing the effective molecular recognition by such an aptasensor as reported previously.[21] However, in the nanopillar configuration, the LOD can be attributed to the nonfaradic current that is proportional to the sensor area and independent of the number of cells on the sensor. To reach single-cell LOD, miniaturization is helpful as the total electrode area without cells is suppressed which reduces the "parasitic" electrical double layer capacitance. In this microelectrodes/microwells configuration, single cells were selectively detected. The florescence microscopy image in Figure 2c shows single Capan-2 cell that was trapped in each microwell (a full fluorescence image of the whole one chip with 20 devices is shown in Figure S5) and the corresponding CVs, as expected, a decrease of I_{peak} (63%) was observed, the absolute I_{peak} value (figures 2c, 2d) for single-cell detection is proportionally reduced compared to the large sensing surface (figures 2a, 2b), which is in the tens of pico-Amperes. A statistical analysis of oxidation I_{peak} of 100 devices (6 chips) for detecting single target cell is depicted in Figure 2e, relative standard deviation (RSD%) is 12.5% (the statistic of reduction I_{peak} and original CVs are shown in Figure S6). Statistic of single non-target cell (Ramos) in 7 chips and relative CVs are performed in Figures 2d, 2f and Figure S5 (RSD% is 23%). Here it is noticed that when there is target cell, the I_{peak} decreased to the limit of background (capacitance) level (Figure 2c, Figure S5a), there is less variation of the current with target cell (Figure 2e), while is the distribution of the histogram of I_{peak} is more broaden with non-target cell, which is crossbonding to different contact

area between the device and each cell because of the heterogeneity. The results indicate that this aptasensor is able be used for single-cell detection and the molecular recognition analysis at single-cell level. To further demonstrate the selectively of the aptasensor device. Figure 3 shows the results of the device working with mixed-cells (50% Capan-2 labelled with green color, and 50% Ramos labelled with red color). After loading the mixed cells and incubated for 30 min (Figure 3a), fresh PBS was flowed to remove the non-trapped cells. By checking the Fluorescence microscopy, it is clear to see that one target cell is on the sensor 1 and one non-target cell is trapped on the sensor 2, as depicted in Figure 3b. The relative CVs with different signal change for the single target cell and single non-target cell in Figures 3c, 3d, indicating the good selectivity of the device in mixed cells. This result showing the promising for granting multi-molecular studies with nanoelectrodes, for instance, interdigitated nanoelectrode,[11] nanowires based aptasensors.[35] Interestingly and significantly, the recent work of atto-Ampere electrochemistry for redox-labelled molecules would be directly beneficial to this EC aptasensor with nano-supported single-cell approach for subcellular sensing.[36] Furthermore, this single-cell array shows the new opportunity for large-scale implementation and statistical analysis of clinical samples, combing our cells filtration method,[8] and the present technology implemented in a 4 inch wafer with $4x10^5$ electrodes that could be used for detecting 1-10 CTC in (1-4)× 10^3 cells.

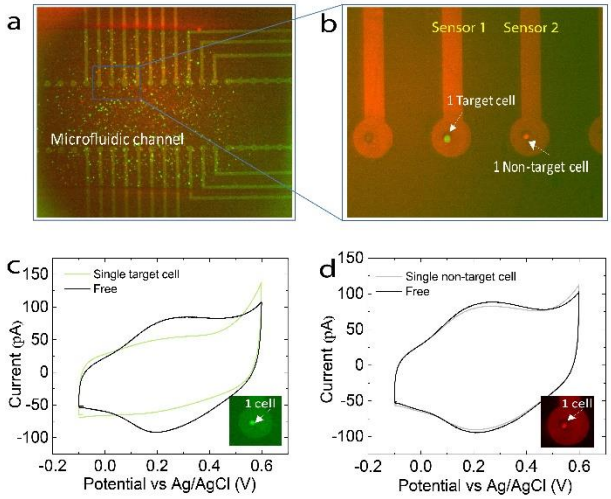

Figure 3. (a) Fluorescent image of mixed cells loaded on the device. (b) Part zoom of (a) to show the single target cell (green) and non-target cell (red) trapped in the microelectrode. (c) CVs (v = 0.05 V/s) in the presence/absence of target cells. (d) CVs (v = 0.05 V/s) of a device in the presence/absence of non-target cells.

In conclusion, an EC aptasensor array with nanopillars was demonstrated for single cancer cell detection. The fabrication approach with nanogap suppresses cell downward force issue on the electrode, that allowing the aptamer moves freely and thereby facilitating the process of molecular recognition. The statistical analysis for nontarget single cell and target single cell shows ultra-sensitivity, selectivity, stability, and reproducibility of the device. This breakthrough method shows outstanding potential for large scale implementation of single-cell arrays, and pushes forward perspectives of using EC devices for further miniaturization at subcellular or single-molecule analysis.

ASSOCIATED CONTENT

Supporting Information available: Experimental and methods, illustration of fabrication of the device, microscopy images of the SU-8 microwells, cell information, additional AFM, additional Fluorescence microscopy images, additional CVs.

AUTHOR INFORMATION

Corresponding Author

* Nicolas Clément, Email: nclement@iis.u-tokyo.ac.jp.
* Shuo Li, Email: shuoli06@iis.u-tokyo.ac.jp.

Present Addresses

†If an author's address is different than the one given in the affiliation line, this information may be included here.

Author Contributions

The manuscript was written through contributions of all authors. All authors have given approval to the final version of the manuscript.

Funding Sources

This work was supported by JSPS Core-to Core Program (JPJSCCA20190006), and the projects "Agence Nationale de la Recherche" (ANR) SIBI(ANR-19-CE42-0011-01), CNRS MITI BIOSTAT, and EU-Attract2 UNICORN-DX project.

ACKNOWLEDGMENT

The authors thank Dr. E. Lebrasseur, Dr. Fujiwara from Takeda CR (Utokyo) for their help and advice with device fabrication, Dr. S. Grall and Dr. L. Jalabert for discussion of the measurement.

Notes

The authors declare no competing financial interest.

REFERENCES

(1) Tellez-Gabriel, M.; Ory, B.; Lamoureux, F.; Marie-Francoise Heymann, M. -F.; Heymann, D. Tumour Heterogeneity: The Key Advantages of Single-Cell Analysis. *Int. J. Mol. Sci.* **2016**, 17, 2142.

(2) Cai, L.; Friedman, N.; Xie, X. S. Stochastic protein expression in individual cells at the single molecule level. *Nature* **2006**, 440, 358-362.

(3) Becht, E.; McInnes, L.; Healy, J.; Dutertre, C. A.; W H Kwok, I.; Lai Guan Ng, L. G.; Ginhoux, F.; W Newell, E. Dimensionality reduction for visualizing single-cell data using UMAP. *Nat. Biotechnol.* **2019**, 37 (1) 38-44.

(4) Shapiro, E.; Biezuner, T.; Linnarsson, S. Single-cell sequencing-based technologies will revolutionize whole-organism science. *Nat. Rev. Genet* **2013**, 14, 618-630.

(5) Navin, N.; Hicks, J. Future medical applications of single-cell sequencing in cancer. *Genome Med.* **2011**, 3, 31.

(6) Xu, X.; Hou, Y.; Yin, X.; Bao, L.; Tang, A.; Song, L.; Li, F.; Tsang, S.; Wu, K.; Wu, H.; et al. Single-cell exome sequencing reveals single-nucleotide mutation characteristics of a kidney tumor. *Cell* **2012**, 148, 886-895.

(7) Miwa, H.; Dimatteo, R.; de Rutte, J.; Ghosh, R.; Di carlo, D. Single-cell sorting based on secreted products for functionally defined cell therapies. *Microsyst. Nanoeng.* **2022**, 8, 84.

(8) Kim, S. H., Ito, H., Kozuka, M., Takagi, H., Hirai, M., Fujii, T., Cancer marker-free enrichment and direct mutation detection in rare cancer cells by combining multi-property isolation and microfluidic concentration. *Lab Chip* **2019**, 19 (5), 757-766.

(9) Nagrath, S., Sequist, L. V., Maheswaran, S., Bell, D. W., Irimia, D., Ulkus, L., Smith, M. R., Kwak, E. L., Digumarthy, S., Muzikansky, A., Ryan, P., Balis, U. J., Tompkins, R. G., Haber, D. A., Toner, M., Isolation of rare circulating tumour cells in cancer patients by microchip technology. *Nature* **2007**, 450 (7173), 1235-1239.

(10) Chennit, K., Trasobares, J., Anne, A., Cambril, E., Chovin, A., Clément, N., Demaille, C. *Anal. Chem.* **2017**, 89 (20), 11061-11069.

(11) Mathew, D. G., Beekman, P., Lemay, S. G., Zuilhof, H., Le Gac, S., van der Wiel, W. G. *Nano Lett.* **2020**, 20 (2), 820-828.

(12) Chennit, K., Coffinier, Y., Li, S., Clément, N., Anne, A., Chovin, A. and Demaille, C., High-density single antibody electrochemical nanoarrays. *Nano Res.* **2022**, Nov 18, 1-7.

(13) Zuo, X. L.; Xiao, Y.; and Kevin W. Plaxco, K. W. High Specificity, Electrochemical Sandwich Assays Based on Single Aptamer Sequences and Suitable for the Direct Detection of Small-Molecule Targets in Blood and Other Complex Matrices. *J. Am. Chem. Soc.* **2009**, 131 (20), 6944-6945.

(14) Downs, A. M.; Plaxco. K., W. Real-Time, In Vivo Molecular Monitoring Using Electrochemical Aptamer Based Sensors: Opportunities and Challenges. *ACS Sens*. **2022**, 7 (10), 2823-2832.

(15) Hansen, J. A.; Wang, J.; Kawde, A. -N.; Xiang, Y.; Gothelf, K. V.; Collins, G. Quantum-Dot/Aptamer-Based Ultrasensitive Multi-Analyte Electrochemical Biosensor. *J. Am. Chem. Soc*. **2006**, 128, 2228-2229.

(16) Demaille, C.; Clément, N.; Chovin, A.; Kim, S. H.; Zheng, Z. The Electrochemical Response of Electrode-Attached Redox OligoNucleotides Is Governed by Low Activation Energy Electron Transfer Kinetics. *ChemRxiv,* December 12, **2022**, DOI: 10.26434/chemrxiv-2022-212hs.

(17) Chao, H., P.; Churcher, Z. R.; Slavkovic, S.; A. Kaiyum, Y., A.; Philip E. Johson, P., E.; Philippe Dauphin-Ducharme, P. Finding the Lost Dissociation Constant of Electrochemical Aptamer-Based Biosensors Erfan Rahbarimehr, *Anal. Chem.* **2023**, 95, 2229-2237.

(18) Zheng Z.; Kim S., H.; Chovin A.; Demaille, C.; Clément, N. Electrochemical response of surface-attached redox DNA governed by low activation energy electron transfer kinetics. *Chem. Sci.* **2023**, DOI: 10.1039/D3SC00320E.

(19) Grall, S.; Li S.; Jalabert L.; Kim S. H.; Chovin, A.; Demaille C.; Clement, N. Electrochemical Shot-Noise of a Redox Monolayer. *arXiv*, **2023**, DOI: 10.48550/arXiv.2210.12943.

(20) Yang, J. M.; Li, X. D.; Jiang, B. Y.; Yuan, R.; and Yun Xiang. In Situ-Generated Multivalent Aptamer Network for Efficient Capture and Sensitive Electrochemical Detection of Circulating Tumor Cells in Whole Blood. *Anal. Chem.* **2020,** 92(11), 7893-7899.

(21) Tran, H., L., Dang, V., D., Dega, N., K., Lu, S., -M., Huang, Y., -F., Doong, R., Ultrasensitive detection of breast cancer cells with a lectin-based electrochemical sensor using N-doped graphene quantum dots as the sensing probe. *Sens. Actuators B. Chem.* **2022**, 368, 132233.

(22) Hempel, F.; Law, J. K. Y.; Nguyen, T. C.; Lanche, R.; Susloparova, A.; Vu, X. T.; Ingebrandt, S. PEDOT:PSS organic electrochemical transistors for electrical cell-substrate impedance sensing down to single cells. *Biosens. Bioelectron.* **2021**, *180*, 113101.

(23) Bonafè, F.; Decataldo, F.; Zironi, I.; Remmondini, D.; Cramer, T.; Fraboni, B. AC amplification gain in organic electrochemical transistors for impedance-based single cell sensors. *Nat. Commun.* **2022**, 13, 5423.

(24) Shen, H. W.; Deng, W. Q.; He, Y. R.; Li, X. R.; Song, J. L.; Liu, R.; liu, H.; Yang, G. Y.; Li, L. Ultrasensitive aptasensor for isolation and detection of circulating tumor cells based on CeO2@Ir nanorods and DNA walker. *Biosens. Bioelectron.* **2020**, 168, 112516.

(25) Luo, J. J.; Liang, D.; Zhao, D.; Yang, M. H. Photoelectrochemical detection of circulating tumor cells based on aptamer conjugated Cu2O as signal probe, *Biosens. Bioelectron*. **2020**, 151, 111976.

(26) Li, S.; Coffinier, Y.; Lagadec, C.; Cleri, F.; Nishiguchi, K.; Fujiwara, A.; Fujii, T.; Kim, S. H.; Clement, N. Redox-labelled electrochemical aptasensors with nanosupported cancer cells. *Biosens. Bioelectron.* **2022**, 216, 114643.

(27) Song, Y.; Zhu, Z.; An, Y.; Zhang, W.; Zhang, H.; Liu, D. Yu, C.; Duan, W.; Yang, C. J. Selection of DNA Aptamers against Epithelial Cell Adhesion Molecule for Cancer Cell Imaging and Circulating Tumor Cell Capture. *Anal. Chem.* **2013**, 85 (8), 4141-4149.

(28) Clement, N.; Patriarche, G.; Smaali, K.; Vaurette, F.; Nishiguchi, K.; Troadec, D.; Fujiwara, A.; Vuillaume, D. Large array of sub-10-nm single-grain Au nanodots for use in nanotechnology. *Small* **2011**, 7 (18), 2607-2613.

(29) Trasobares, J.; Rech, J.; Jonckheere, T.; Martin, T.; Aleveque, O.; Levillain, E.; Diez-Cabanes, V.; Olivier, Y.; Cornil, J.; Nys, J. P.; Sivakumarasamy, R.; Smaali, K.; Leclere, P.; Fujiwara, A.; Theron, D.; Vuillaume, D.; Clement, N. A 17 GHz molecular rectifier. *Nat. Commun.* **2016**, 7, 12850.

(30) Anne, A.; Demaille, C. Dynamics of Electron Transport by Elastic Bending of Short DNA Duplexes. Experimental Study and Quantitative Modeling of the Cyclic Voltammetric Behavior of 3`-Ferrocenyl DNA End-Grafted on Gold. *J. Am. Chem. Soc.* **2006**, 128, 542-557.

(31) Steentjes, T.; Jonkheijm, P.; Huskens, J. Electron Transfer Processes in Ferrocene-Modified Poly(ethylene glycol) Monolayers on Electrodes. *Langmuir* **2017**, 33 (43), 11878-11883.

(32) Dauphin-Ducharme, P.; Arroyo-Currás, N.; Adhikari, R.; Somerson, J.; Ortega, G.; Makarov, D. E.; Plaxco, K. W. Chain Dynamics Limit Electron Transfer from Electrode-Bound, Single Stranded Oligonucleotides. *J. Phys. Chem. C* **2018**, 122 (37), 21441-21448.

(33) Xie, X.; Li, F.; Zhang, H.; Lu, Y.; Lian, S.; Lin, H.; Gao, Y.; Jia, L. EpCAM aptamer-functionalized mesoporous silica nanoparticles for efficient colon cancer cell-targeted drug delivery. *Eur. J. Pharm. Sci*. **2016**, 83, 28-35.

(34) Mayado, A.; Orfao, A.; Mentink, A.; Gutierrez, M. L.; Muñoz-Bellvis, L. Terstappen, L. W. M. M. Detection of circulating tumor cells in blood of pancreatic ductal adenocarcinoma patients. *Cancer Drug Resist.* **2020**, 3, 83-97.

(35) Grall, S., Alic, I., Pavoni, E., Awadein, M., Fujii, T., Mullegger, S., Farina, M., Clément, N., Gramse, G. Attoampere nanoelectrochemistry. *Small* **2021**, 17 (29), 2101253.

(36) Kutovyi, Y., Hlukhova, H., Boichuk, N., Menger, M., Offenhäusser, A., Vitusevich, S., Amyloid-beta peptide detection via aptamer-functionalized nanowire sensors exploiting single-trap phenomena. *Biosens. Bioelectron.* **2020**, 154, 11205.